Experimental and Theoretical Investigations on the Epitaxial Growth of 4,4′ stilbenedicarboxylic acid molecules on Au(111)

doi: 10.1063/1.3256288

Experimental and theoretical investigations on the epitaxial growth of 4,4′ stilbenedicarboxylic acid molecules on Au(111)

Yan Feng Zhang,[1] Yong Yang,[2] Yoshiyuki Kawazoe,[2] and Tadahiro Komeda[1,3,a)]
[1]*Institute of Multidisciplinary Research for Advanced Materials, Tohoku University, Katahira 2-1-1, Aoba-ku, Sendai 980-8577, Japan*
[2]*Institute for Materials Research, Tohoku University, Katahira 2-1-1, Aoba-ku, Sendai 980-8577, Japan*
[3]*CREST, JST, Honcho 4-1-8, Kawaguchi-shi, Saitama 332–0012, Japan*

(Received 5 May 2009; accepted 28 September 2009; published online 5 November 2009)

We report on scanning tunneling microscope observations of the epitaxial growth of 4,4′ stilbenedicarboxylic acid (SDA) molecules on Au(111), with the coverage ranges from submonolayer to one monolayer. The surface assembly evolves from one-dimensional molecular chains to striped islands and finally monolayer films. For two-dimensional assembly, the head-to-tail hydrogen bonding is found to dominate the molecule-molecule interactions. Each linking region of the SDA molecular chains consists of two hydrogen bonds. This is confirmed by our first-principles calculations where the hydrogen bond length, hydrogen bond energy, and SDA-Au interaction energy are deduced theoretically. Moreover, the configurations with interchain hydrogen bonds are energetically unstable. The roles of the herringbone reconstruction of Au(111) and the compression effect of a complete film on the formation of molecular ribbons are discussed. © *2009 American Institute of Physics*. [doi:10.1063/1.3256288]

I. INTRODUCTION

Low dimensional supramolecule architectures, stabilized by noncovalent links such as hydrogen bonding and donor-acceptor and metal-ligand interactions, attracted wide attention in designing complex nanosystems with molecular building blocks.[1–3] Among these studies, supramolecule assembly combined with hydrogen bonding formation has been proven to be a promising approach for the fabrication of unique molecular materials.[4–10] The selection of building blocks with appropriate functional groups should play important roles in tuning the geometrical and chemical properties of two-dimensional (2D) assemblies. On the other side, the chemical reactivity and the geometrical symmetry of the substrate should introduce strong influences on the molecular assembly. Thus, to control the fabrication of supramolecules, it is critical to understand (1) molecule-molecule interactions through their functional groups, (2) molecule-substrate interactions, and (3) balance of these two interactions.

Supramolecules assembly through hydrogen bonding between carboxylic groups have been studied extensively in recent years.[11–13] The assembly of terephthalic acid (TPA) on Cu(100) was researched with various surface sensitive analysis methods where the thermal effect activated deprotonation of carboxylic groups was explained to be a decisive factor for the fabrication of a square lattice.[14] Similar results were reported in 4-4′-biphenyl dicarboxylic acid (BDA) and stilbenedicarboxylic acid (SDA) assembly on Cu(100).[15] In this research, the symmetry difference between BDA and SDA can be reflected in the supramolecule assembly. On an inert and reconstructed Au(111) surface, the assemblies of TPA molecules were observed to be mainly dominated by a head-to-tail one-dimensional (1D) hydrogen dimer formation.[16] A similar case was also addressed in the assembly of BDA /Au(111).[10]

In this work, we report on scanning tunneling microscope (STM) observations in combination with first-principles calculations for the epitaxial growth of SDA molecules on the reconstructed Au(111) surface. Different from the straight-line TPA and BDA molecules, the SDA molecules have a bend in the middle. Meanwhile, the Au(111) substrate is an inert template with low chemical reactivity, on which the carboxylic groups can be kept intact and free from deprotonation. The reconstructed substrate can also provide natural dislocation patterns that regulate the interatomic interactions in a periodic manner. This can be an ideal template to study the long-range modulations of substrate on the hydrogen bonding geometry. A comparison can also be made between the surface assembly of SDA on Au(111) and Cu(100).

II. METHOD SECTION

A. Scanning tunneling microscope

The experiment was carried out with a home-built STM which was placed in a UHV chamber with a base pressure better than 4×10^{-10} mbar. The Au(111) substrate was prepared by a standard method of Ar^+ sputtering followed by annealing at 600□ for half an hour. The $(22\times\sqrt{3})$ reconstructed surface of Au(111) was then confirmed by our STM observations. 4-4′ SDA molecules (Wako, Japan, ≥96%) were degassed by heating a Ta container for several hours in

a)Author to whom correspondence should be addressed. Electronic mail: komeda@tagen.tohoku.ac.jp. Present address: Institute of Multidisciplinary Research for Advanced Materials, Tohoku University, Katahira 2-1-1, Aoba-ku, Sendai 980-8577, Japan. Tel.: +81 22 2175368. FAX: +81 22 2175404.

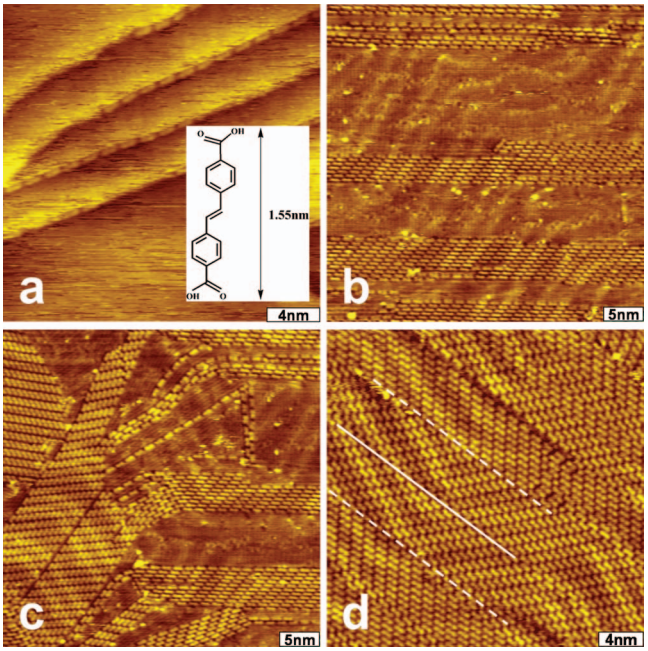

FIG. 1. [(a)–(d)] STM topographies (V=−0.5 V, I=0.4 nA) of SDA assembly on Au(111), with coverage of 0.1, 0.4, 0.7, and 0.9 ML, respectively. The inserted plot in (a) shows the structure of SDA. The resulted surfaces are characterized with single or double molecular rows, striped phases, and continuous molecular ribbons. The herringbone structure of Au superimposes on the 2D phase in (d). The dashed lines indicate the boundaries of some molecular ribbons.

prior to evaporation. The following deposition was done with a flux rate of ~0.1 ML per minute, which was calibrated by reading an *in situ* thickness monitor. The sample was transferred instantly to the STM chamber. All the STM measurements were conducted subsequently in the UHV condition with the sample kept at room temperature.

B. *Ab initio* simulations

It is self-evident that the intermolecular bonding between the SDA molecules plays a key role in determining the morphology of SDA assemblies on Au(111). However, the information regarding the bonding structures is hard to extract from the STM images because of the resolution limit. Thus, we recourse to *ab initio* simulations, state-of-the-art the most accurate methods to treat atom-atom interactions. The computational details are provided in the online supplemental material.[17]

III. RESULTS AND DISCUSSION

The structure of a SDA molecule is schematically shown in the inset of Fig. 1(a), in which two benzene rings are connected by an ethenylene bridge, with carboxylic groups at both ends. The length of the molecule is ~15.5 Å measured along the long axis direction. The STM images showing the SDA assembly on Au(111) are displayed in Figs. 1(a)–1(d), where the evolutions of surface morphologies with the increase IN coverage are obtained. In these images, the bright elongated protrusions of ~15 Å in axial length should correspond to the flat lying geometry of SDA molecules. This

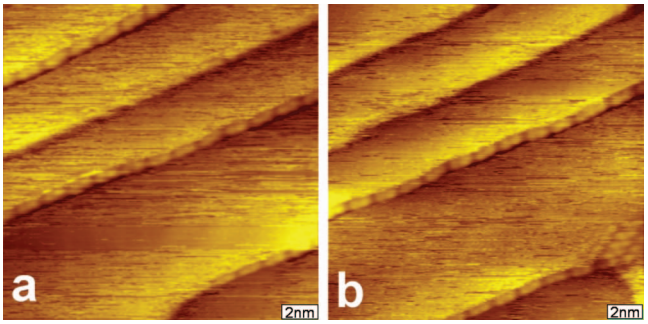

FIG. 2. (a) 1D SDA chains elongated along Au(111) step edges. (b) Similar surface obtained after several repetitive scanning of (a). The STM images were taken under a tunneling condition of V=−0.6 V, I=0.4 nA.

configuration also compares well with the bonding characteristics of aromatic species on metal surfaces.[14–16,18]

At low concentrations, SDA molecules are expected to be mobile on the Au(111) surface due to the thermal diffusion, and individual molecules may not be imaged on the terraces within a room temperature observation. This assumption can be verified by our experiments, where SDA molecules tend to form 1D chains along the step edges of Au [Fig. 1(a)]. With the coverage increasing to ~0.4 ML, the adsorbed molecules prefer to form ordered domains with sharp boundaries [Fig. 1(b)]. These 2D domains can be regarded as an accumulation of parallel 1D chains.

The surface assembly manifests a versatile feature if we further increase the coverage. In Fig. 1(c) at coverage of ~0.7 ML, 1D chains, double or triple molecular rows, and stripped islands can coexist on a same surface with different orientations. The multiorientations of the molecular assemblies may reflect weak SDA-Au(111) interactions. The dashed lines in Fig. 1(d) are used to separate a complete thin film into several ribbons. Since around the dashed lines, the long range ordering of the film is broken. In this case, we can define a 2D phase possessing an identical 1D chain orientation and interchain direction as a ribbon. Each ribbon is usually composed of more than ten parallel rows. If each ribbon is regarded as a general, they can be arranged with a phase shift or in mirror symmetries.

The molecule-molecule interactions are usually explained to be derived from the head-to-tail hydrogen bonding formation between carboxylic acids molecules, as seen in the growth of TPA and BDA on Au(111).[10,16] For SDA/Au(111), we first consider the alignment of the molecules along the step edges of Au. In Fig. 2(a), we show a magnified STM image of the SDA rows. Since Au step edges usually contain a microscopic roughness from a perfect straight line, the molecules accumulated along the step edges tend to develop crooked rows. In this way, the end groups of carboxylic should be active in bonding with neighboring molecules by the formation of hydrogen bonds. By a repetitive scanning of the area shown in Fig. 2(a), we can notice the missing of an entire chain and the formation of a small island at the lower right corner [Fig. 2(b)]. The high mobility of SDA molecules may indicate weak SDA-SDA interactions inside a 1D chain.

The formation of 2D domains is shown in Fig. 3(a) with its magnified image displayed in Fig. 3(b). With this image,

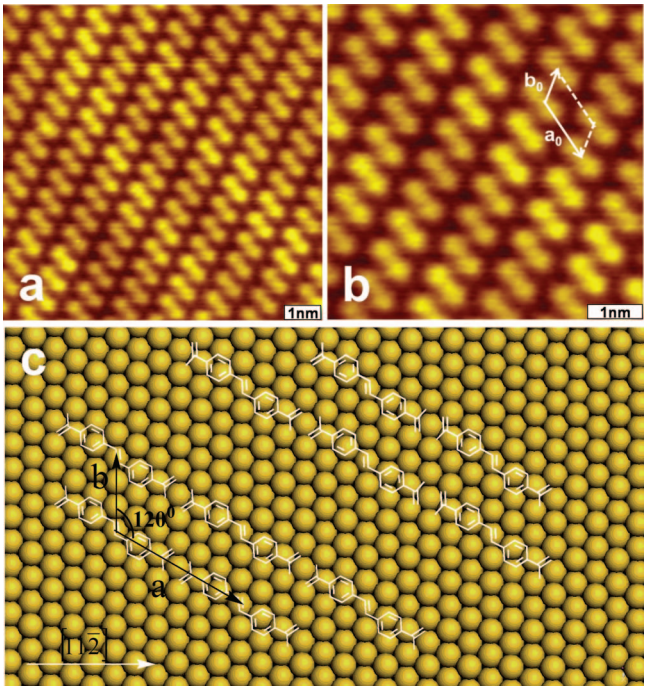

FIG. 3. [(a) and (b)] Close-view images (V=−0.4 V, I=0.4 nA) of SDA assembly on Au(111). The vectors of $\boldsymbol{a_0}$ and $\boldsymbol{b_0}$ indicate the period along the 1D chain direction and the nearest neighboring direction, respectively. (c) Tentative models accounting for molecule-molecule interactions through a head-to-tail hydrogen dimer formation, with **a** and **b** indicating the unit vectors. Two types of enantiomers were provided by considering a prochiral character of the molecule.

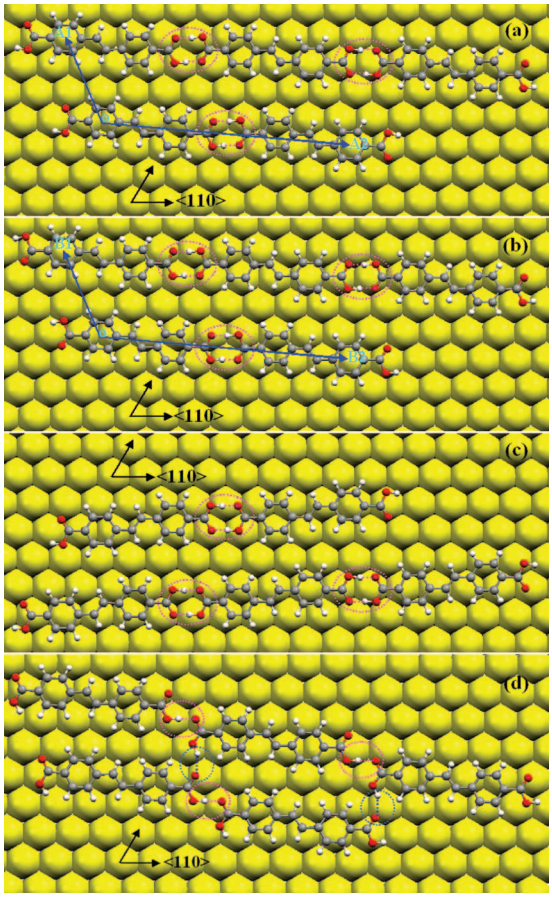

FIG. 4. [(a)–(c)] Simulation models for three types of SDA stereoisomer on Au(111) with the head-to-tail paring hydrogen bonded configurations. OA1 and OB1 point to interchain directions, while OA2 and OB2 illustrate the chain orientations. Specially, the SDA molecules in models (b) and (c) are enantiomers of each other. (d) Another possible configuration with both intrachain and interchain hydrogen bonding geometries. All the hydrogen bonds are denoted by dotted lines and included in dashed circles.

we can determine the overlayer lattice experimentally. The periodicity along the chain orientation [labeled with $\boldsymbol{a_0}$ in Fig. 3(b)] is measured to be $\sim 16.4 \pm 0.2$ Å, which is the distance between the centers of the adjacent molecules from the same chain. The inter-row period $\boldsymbol{b_0}(\sim 8.3 \pm 0.2$ Å) is calculated from the centers of two molecules from neighboring chains. The two vectors of $\boldsymbol{a_0}$ and $\boldsymbol{b_0}$ are rotated by $\sim 120°$ with each other. On average, there is one SDA molecule enclosed in the 2D periodic surface cell as constructed by the vectors $\boldsymbol{a}$ and $\boldsymbol{b}$ [Fig. 3(b)]. The area of the surface unit cell is $S=|\vec{a}\times\vec{b}|=|\vec{a}||\vec{b}|\sin(\pi/3)=117.88$ Å^2. Consequently, the density of SDA molecules on the Au(111) is $\sim 1/(117.88$ Å$^2) \sim 8.5\times 10^5/\mu$m^2.

To explain the molecule-molecule interactions, a tentative model is proposed in Fig. 3(c), in which the molecule chains are orientated along the close-packed direction of Au. One carboxylic group from an SDA molecule will interact with the carboxyl group of the other molecule in the same chain. In this way, a head-to-tail hydrogen bonding geometry is established.

Similar to Fig. 3(b), we define two unit vectors that determine the 2D ordering. In Fig. 3(c), $\boldsymbol{a}$ is along the 1D chain direction and $\boldsymbol{b}$ points to the molecule in the adjacent chain. These two vectors are rotated by $\sim 120°$ with each other. The absolute length of $\boldsymbol{a}$ and $\boldsymbol{b}$ are $\sim 6c_0$ and $\sim 3c_0$, respectively, where c_0 is the Au(111) lattice constant (~ 2.75 Å). As the distance between the two O atoms in the carboxyl groups from both ends of a SDA molecule is ~ 13.6 Å, the hydrogen bond length (the O–O distance) can be deduced to be $\sim 2.8 \pm 0.2$ Å. This value agrees well with the typical hydrogen bonding length reported for several carboxylic molecules adsorbed on metal surfaces.[10–16]

The bonding structures of SDA chains, and the validity of the model suggested in Fig. 3(c), are further proved by our first-principles calculations. The (10×5) surface cell of a one-layer Au sheet is used to model the Au(111) substrate. Four adsorption models are considered, as shown in Figs. 4(a)–4(d). We first examine the head-to-tail linked SDA chains, in which two hydrogen bonds present in each linkage site. In the three models shown in Figs. 4(a)–4(c), the SDA molecules are stereoisomers of each other. In particular, the SDA molecules shown in Fig. 4(c) are enantiomers of the ones in Fig. 4(b), and the model in Fig. 4(c) can be obtained via mirror reflection of Fig. 4(b) about the Au(110) plane. The model in Fig. 4(d) assumes an interchain hydrogen bonding geometry.

The SDA-Au bonding energy is ~ 0.1 eV/SDA, with a separation of ~ 3.3 Å between the benzene plane and the Au(111). The calculated SDA-SDA interacting energies, hydrogen bonding energies, the separations of O–O and O–H in the hydrogen bonds are given in Table I. Our calculation shows that the strength of hydrogen bonds in Figs. 4(a) and

TABLE I. The SDA-SDA interaction energies, the averaged hydrogen bonding energies and O–O and H–O distances (proton to its O acceptor) of hydrogen bond obtained by our calculations. For Figs. 4(a)–4(c), the number of SDA (N_{SDA}) in the simulation cell is 5, while the number of hydrogen bond (N_{HB}) is 6, thus $E_{H\text{-}Bond} \sim E_{SDA\text{-}SDA} \times 5/6$. For Fig. 4(d), $N_{SDA}=N_{HB}$, so $E_{H\text{-}Bond} \sim E_{SDA\text{-}SDA}$. The distances are averaged values with standard deviation given in parentheses. In the case of Fig. 4(d), two types of hydrogen bond are present with different bonding lengths.

Configuration	$E_{SDA\text{-}SDA}$ (eV)	$E_{H\text{-}Bond}$ (eV)	d_O···O (Å)	d_H···O (Å)
Figure 4(a)	0.48	0.40	2.52(1)	1.47(1)
Figure 4(b)	0.48	0.40	2.51(1)	1.44(1)
Figure 4(c)	0.48	0.40	2.51(1)	1.44(1)
Figure 4(d)	0.31	0.31	2.60(1); 2.89(3)	1.57(1); 2.00(5)

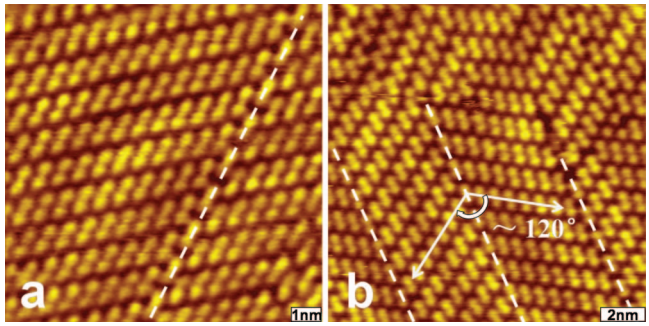

FIG. 5. [(a) and (b)] STM images (V=−0.4 V, I=0.4 nA) of the formation of continuous ribbons inside an SDA film. The dashed lines indicate the boundaries of the ribbons.

4(b) is the same (~0.4 eV). In these two configurations, the hydrogen bonding geometries are also very close to each other, which are indicated with dashed circles in corresponding figures. This means that both adsorption structures should have the same probability of being observed experimentally. As for Fig. 4(c), our DFT calculations give the same structural and energetic parameters as that in Fig. 4(b). This is due to the fact that the Hamiltonian that governs the energetics of the system is invariant under symmetry operations such as mirror reflection. Apparently, the relative positions of all the atoms in Fig. 4(c), such as bond lengths, bond angles, and coordination numbers are kept the same as Fig. 4(b). Moreover, for different chain orientations, few changes are expected for the structural and energetic parameters because of the weak SDA-Au(111) interactions. Similar conclusion applies to the enantiomer chains of the SDA in Fig. 4(a), and more generally to the enantiomer chain of any organic molecules. In fact, the result discussed here, i.e., the mirror reflection invariance of the energetics of the system investigated is a consequence of the parity conservation in electromagnetic interactions.[19]

In contrast, the configuration shown in Fig. 4(d) is energetically less favored, because of its smaller hydrogen bonding energy. Moreover, the SDA molecules in Fig. 4(d) are less stable than the upper three cases [Figs. 4(a)–4(c)], due to their higher internal energies (differs by ΔE_{SDA} ~0.27 eV/molecule). Considering the periodic nature, there are two hydrogen bonds and one SDA in each unit cell. Thus, at temperature T, the probability ratio for finding the adsorption configuration shown in Fig. 4(d), and the ones shown in Fig. 4(a) [or Figs. 4(b) and 4(c)] is calculated as follows:

$$P_A(\text{or } P_B, P_C)/P_D \sim \exp[-\Delta E/k_B T] = \exp[-(\Delta E_{SDA} + 2\Delta E_{H\text{-}Bond})/k_B T], \quad (1)$$

where k_B is the Boltzmann constant. With $\Delta E_{SDA}=0.27$ eV, $\Delta E_{H\text{-}Bond}=0.09$ eV, and $T=300$ K, the ratio is deduced to be $\sim 2.8\times 10^{-8}$. At such a low probability, it is almost impossible to observe interchain hydrogen bonding configurations in SDA patterns. On the contrary, the head-to-tail hydrogen bonding should dominate the molecule-molecule interactions in 2D assembly.

In Figs. 4(a) and 4(b), the orientation of 1D chains can be coordinated by two vectors joining the centers of benzene rings: OA1 and OA2 for Fig. 4(a) and OB1 and OB2 for Fig. 4(b). The lengths of OA1 and OB1 are calculated to be 8.46 and 8.48 Å, which agree well with the experimental value (~8.31 Å). The angle formed between the two orientation vectors is 119.78° for Fig. 4(a) and 119.60° for Fig. 4(b). Again, they coincide well with the experimental data (~120°). We can also notice that the base vectors of the unit cell are oriented slightly from the high symmetry directions of Au, as suggested in Fig. 3(c).

The O–O distances of the hydrogen bonds in both Figs. 4(a) and 4(b) are calculated to be ~2.5 Å, which is a little bit smaller than the value estimated by STM measurements (~2.8±0.2 Å). This discrepancy may be explained by further improving the theoretical calculation accuracy accompanied by imaging the surface with an even higher resolution STM.

This SDA/Au(111) is much different from SDA/Cu(100), where the hydrogen bonding is described to be between a carboxylate group and a benzene hydrogen or an ethenylene hydrogen.[15] Our Au(111) substrate is proved to be a more inert surface and no deprotonation effect happens. In large-scale STM images, we can find several domains on a same surface with their orientations rotated by a multiple of ~60° with each other. These selective orientations of SDA domains can be regarded as a reflection of the threefold symmetry of Au(111).

Interesting "ribbonlike" structures appear when the SDA coverage reaches one monolayer (Fig. 5). The molecular chains from the lower right part show a positional shift from that of the upper left side at the domain boundary, as indicated by the dashed line in Fig. 5(a). Figure 5(b) demonstrates a case where neighboring ribbons are arranged in mirror symmetries.

Above the continuous molecule ribbons, the reconstructions of Au(111) can be clearly observed on SDA layers [Fig. 5(b)]. It is easy to think that the herringbone structure of Au should be considered to be a partial driving force. Since around the dislocation lines, the bonding configurations of SDA molecules could be changed, in order to adjust the adsorption sites of aromatic rings on the threefold hollow sites of Au(111).[16,18] In addition, the ribbons usually posses a size of 7–12 molecular rows, as is comparable with the dimension of the substrate reconstruction of a scale of ~6 nm.

Another important factor may be the compression of the

layer upon approaching one monolayer, which will result in the separation of a 2D film into some ribbonlike domains. This assumption was confirmed by our further coverage dependent STM examinations. A minimum coverage of 0.90 ML was found to be the critical value for the formation of long-range continuous ribbons. Below this coverage, SDA domains with different orientations can be accumulated [Fig. 1(c)].

IV. SUMMARY

We studied the surface assembly of SDA molecules on the reconstructed Au(111) surface by using STM. The driving force for the 2D assembly is expected to be dominated by the typical head-to-tail hydrogen dimer formation. This assumption is further verified by our first-principles calculations, where the chain orientation, the interchain direction, the hydrogen bond energy, and bond length are deduced. The results compare well with our experimental data and give more insights into the molecule-molecule interactions and adsorption structures in the 2D assembly. Moreover, our calculations show that the configurations with interchain hydrogen bonds are energetically much unstable and of little possibility of being observed experimentally. The multiorientations of the coexisting domains can be explained by the threefold symmetry of the substrate, and the weak SDA-Au(111) interactions. In addition, the substrate effect from the herringbone reconstruction and the compression effect of a complete film are expected to be the reasons for the formation of ribbons in a near complete SDA film.

ACKNOWLEDGMENTS

This research was partially supported by the Ministry of Education, Science, Sports and Culture, Grant-in-Aid for Scientific Research on Priority Areas, 448, 2005. Y.F.Z acknowledges the financial support of the Japan Society for the Promotion of Science (JSPS). Y.Y. and Y.K. are grateful to the staff of the Center for Computational Materials Science at Institute of Materials Research of Tohoku University.

[1] J. M. Lehn, Proc. Natl. Acad. Sci. U.S.A. **99**, 4763 (2002).
[2] V. Balzani, A. Credi, F. M. Raymo, and J. F. Stoddart, Angew. Chem., Int. Ed. Engl. **39**, 3349 (2000).
[3] D. N. Ed. Reinhoudt, *Supramolecule Materials and Technologies* (Wiley, Chichester, 1999).
[4] J. V. Barth, J. Weckesser, C. Cai, P. Gunter, L. Burgi, O. Jeandupeux, and K. Kern, Angew. Chem., Int. Ed. **39**, 1230 (2000).
[5] T. Kawai, H. Tanaka, and T. Nakagawa, Surf. Sci. **386**, 124 (1997).
[6] T. Yokoyama, S. Yokoyama, T. Kamikado, Y. Okuno, and S. Mashiko, Nature (London) **413**, 619 (2001).
[7] Q. Chen and N. Richardson, Nature Mater. **2**, 324 (2003).
[8] J. A. Theobald, N. S. Oxtoby, M. A. Philips, N. R. Champness, and P. H. Beton, Nature (London) **424**, 1029 (2003).
[9] A. Dmitriev, N. Lin, J. Weckesser, J. V. Barth, and K. Kern, J. Phys. Chem. B **106**, 6907 (2002).
[10] N. Zhu, T. Osada, and T. Komeda, Surf. Sci. **601**, 1789 (2007).
[11] T. Thundat, R. J. Warmack, D. P. Allison, and T. L. Ferrell, Ultramicroscopy **42–44**, 1083 (1992).
[12] Y. Ishikawa, A. Ohira, M. Sakata, C. Hirayama, and M. Kunitake, Chem. Commun. (Cambridge) **2002**, 2652 (2002).
[13] G.-J. Su, H.-M. Zhang, L.-J. Wan, C.-L. Bai, and T. Wandlowski, J. Phys. Chem. B **108**, 1931 (2004).
[14] S. Stepanow, T. Strunskus, M. Lingenfelder, A. Dmitriev, H. Spillmann, N. Lin, J. V. Barth, Ch. Woll, and K. Kern, J. Phys. Chem. B **108**, 19392 (2004).
[15] S. Stepanow, N. Lin, F. Vidal, A. Landa, M. Ruben, J. V. Barth, and K. Kern, Nano Lett. **5**, 901 (2005).
[16] S. Clair, S. Pons, and A. P. Seitsonen, H. Brune, K. Kern, and J. V. Barth, J. Phys. Chem. B **108**, 14585 (2004).
[17] See EPAPS supplementary material at http://dx.doi.org/10.1063/1.3256288 for the details of the DFT calculation.
[18] J. V. Barth, J. Weckesser, G. Trimarchi, M. Vladimirova, A. De. Vita, C. Z. Cai, H. Brune, P. Gunter, and K. Kern, J. Am. Chem. Soc. **124**, 7991 (2002).
[19] C. N. Yang, Science **127**, 565 (1958).